

Wood derived hard carbon anode material for low-cost sodium-ion batteries towards practical application for grid energy storage

Ş. Patat^{1,2*}, A. Ülgen¹, S. Yıldız^{1,2}, A. R. Türkmen¹, T. Öztürk²

¹Erciyes University Faculty of Science, Department of Chemistry, Kayseri/Turkey

²ENDAM, Middle East Technical University, Ankara, Turkey

Electrochemical performance of the hard carbon derived from pine wood pyrolyzed at the temperature of 1600°C for 2 h is investigated as an anode material for sodium ion batteries. The synthesized hard carbon is characterized by X-ray diffraction, field-emission scanning electron microscopy equipped with energy dispersive x-ray spectrometry (EDX), nitrogen adsorption sorptometry, Raman spectroscopy, and conductivity measurements. The yield of hard carbon is 21%, based on the weight of precursor. The hard carbon demonstrates a low irreversible capacity of 26%, the reversible capacity of 234 mA h g⁻¹ at a current density of 30 mA g⁻¹, and a capacity retention of ~96.2% after 134 cycles at 1C.

Keywords: Hard carbon, sodium ion batteries, energy storage systems

INTRODUCTION

Energy storage systems have very important role in the development of portable electronic devices, electric vehicles and large-scale electrical energy storage applications for renewable energy, such as wind and solar power. Lithium ion batteries have dominated the market for portable electronic devices and electric vehicles due to the highest energy density and long cycle life. Sodium ion batteries have attracted great interest recently, especially for grid-scale energy storage because of the cheap, democratic global distribution and abundant of sodium resources [1]. Despite this, the absence of a suitable anode material limits their development. Graphite is the most widely used anode material in commercial lithium ion batteries owing to its abundant resource, excellent electronic conductivity, reasonable reversible capacity (up to 372 mAh g⁻¹), low and flat potential plateaus, high Coulombic efficiency, outstanding cycling stability, and low cost. Unfortunately, graphite demonstrates poor electrochemical performance as an anode material for sodium ion batteries using traditional carbonate electrolytes, mainly attributed to the larger ionic radii of the Na versus Li (102 Å versus 0.76 Å). The candidate anode materials for sodium ion batteries can be classified into carbonaceous materials, alloys, oxides and organic compounds [2, 3]. Among these candidates, hard carbon is one of the most promising anode materials for sodium ion

batteries because of its high specific capacity, low cost, low average potential and facile preparation methods [4]. Therefore, developing a high-performance hard carbon anode is highly desirable. However, hard carbon anodes suffer from the low initial Coulombic efficiency, the poor rate and the poor cycling performance due to side reactions related to larger surface area resulting from the nanostructures. To improve the initial Coulombic efficiency, cycling stability and rate performance, two kinds of methods have been used. One way is the surface modifying to reduce the contact area of carbon anode with electrolyte, which cause low initial Coulombic efficiency [5, 6]. The other one is to optimize the electrolyte [7]. Although some sodium can be trapped in hard carbon anode leading to the initial Coulombic efficiency loss, it is generally considered that hard carbon with a low surface area can give a high initial Coulombic efficiency [6]. It is found that the plateau capacity at the low potential region of voltage profile increases with increasing the carbonization temperature and the insertion process of Na into closed nanovoids limits the rate performance [8]. However, reducing the cost and minimizing the surface area of hard carbon remain a significant challenge. Cellulose is the most abundant and also renewable resource on Earth, which has attracted great interest as a carbon precursor. Various biomasses, such as wood [9-11], mangosteen shell [12], spinifex [13], sucrose [14-16], paper pulp mill sludge [17], banana peel [18], orange peel [19], peat moss [20], and pomelo peels [21] and peanut shell [22] have been used as

* To whom all correspondence should be sent:
patat@erciyes.edu.tr

precursors and the hard carbons derived from them show good performance as anode for sodium ion batteries. In this work, hard carbons derived from pine wood have been successfully developed as anodes for sodium ion batteries.

EXPERIMENTAL SECTION

Hard Carbon Synthesis

The collected pine wood was washed with deionized water, cut into small pieces, and dried at 110°C overnight in an oven. Typically 10 g of wood precursor was loaded in a tube furnace and heated at 1600°C for 2h under an argon atmosphere with the flow rate of 100 sccm. The obtained carbon was ground using ball mill at 350rpm for 1h before use.

Materials Characterization

The crystallinity and the phases of the hard carbon samples were identified by powder X-ray diffraction (XRD) using copper $\text{CuK}\alpha$ radiation ($\lambda=1.5406 \text{ \AA}$) (Bruker AXS D8). The X-ray powder diffraction measurements were made using a Bruker AXS D8 X-ray diffractometer equipped with copper X-ray tube, NaI type scintillation counter detector and graphite monochromator. The diffraction data were collected in 2θ range of 10° - 70° with the step size of 0.02° and a count time of 10 s per step at 40 kV and 40mA.

The Raman spectra were recorded with a confocal microprobe Raman system (Thermo Nicolet Almega XR Raman microscope). The surface morphology of the samples was investigated using a scanning electron microscope (SEM, LEO 440), operated at an accelerating voltage of 20 kV, equipped with energy dispersive X-ray spectrometry (EDX). The samples were laid on carbon tape before being measured and covered with Au-Pd alloy under high vacuum. The elemental composition of the samples was determined by EDX.

The conductivities of the samples were measured at room temperature by linear scanning voltammetry. The powder samples were uniaxially pressed into pellets under a pressure of about 9 tons using a stainless steel die with 13 mm diameter. The prepared pellets were located in a two-electrode Swagelok type cell and the potential versus current values were measured in a potential range of 0-100 mV at a scanning speed of $5 \text{ mV}\cdot\text{s}^{-1}$ with AMETEK Princeton Applied Research VersaSTAT MC model multi-channel galvanostat/potentiostat.

The conductivity is calculated from the slope (V/I) of current versus potential curve given in Eq. (1):

$$\frac{V}{I} = R, \rho = R \cdot \frac{s}{l} \text{ ve } \chi = \frac{1}{\rho} = \frac{l}{sR} \quad (1)$$

Where V, I, R, ρ , s, l, and χ stand for voltage (mV), current (mA), the resistance (ohm), resistivity (ohm.cm), the surface area of pellet (cm^2), thickness of pellet (cm), and conductivity (S/cm), respectively.

Nitrogen adsorption/desorption isotherms of the hard carbon materials were measured using nitrogen gas adsorption on Micromeritic Corporation TriStar II 3020 V1.03. Before measurements, the samples were degassed for 24 hours at 120 °C. Once degassed, the isotherms were measured at 77 K in a p/p^0 (relative pressure) range of 0.001-1, with P^0 being 760 torr. The specific surface area and the pore size distribution were calculated with the Brunauer-Emmett-Teller (BET) and the Barrett-Joyner-Halenda (BJH) methods, respectively.

Electrochemical Characterization

For preparation of the working electrodes, the hard carbon powders (96 wt%) were mixed with sodium alginate (Sigma-Aldrich) as a binder (4 wt%) in *deionized water*. The obtained slurry was pasted onto a piece of Al foil with doctor blade, followed by drying at 60°C in air for 3h, roll pressing, drying at 120°C for 10h in a vacuum oven, and cutting into 13 mm disks, respectively prior to use. The active material mass loading of the electrode ranged from 6 to 8 mg cm^{-2} . A three electrode Swagelok type electrochemical cell with the electrode diameter of 13 mm was used to measure the electrochemical performance. The cell was assembled in an Ar filled glove-box using the hard carbon as a working electrode, pure sodium metal disks (Merck) both as a counter and a reference electrode, a glass fiber filter as a separator and 1M NaPF_6 (Sigma-Aldrich) in 1:1 by weight ethylene carbonate (Merck) and propylene carbonate (Merck) as the electrolyte. The constant current charge/discharge measurements were carried out in the potential range of 0.01-3.0V at different current densities ranging from 0.1C to 1C ($1\text{C}=300 \text{ mA g}^{-1}$) on an AMETEK Princeton Applied Research VersaSTAT MC model multi-channel galvanostat/potentiostat. The cycle life stability was studied by using constant current charge/discharge measurements in the potential

range of 0.01V-3.0V at 1C for 100 cycles. All electrochemical tests were conducted at room temperature.

RESULTS AND DISCUSSION

The elemental content of the hard carbon determined by EDX is found to be 93.73 at % C, 5.39 at%O, 0.40 at% Ca, 0.21 at% Fe and 0.26 at % K. Its conductivity is measured to be 0.73 S cm⁻¹. Its X-ray diffraction (XRD) pattern is given in Fig.1. The XRD pattern demonstrates two broad peaks at ~24° (revealing the non-graphitic nature) and ~44°, which are assigned to the crystallographic planes of (002) and (100) in the carbon structure, respectively. On the basis of the Bragg equation $2d \sin \theta = n\lambda$, the d_{002} value of the hard carbon is 0.371nm, which is much larger than that of graphite (~0.340nm), leading to facile sodium-ion insertion/extraction between the graphene layers. The thickness (L_c) and average width (L_a) of the graphitic domains are calculated using the Scherrer equation with the peak positions and full width at half maximum (FWHM) values of (002) and (100) peaks at $2\theta \approx 24^\circ$ and $2\theta \approx 44^\circ$, respectively. According to the d_{002} and L_c values, the number of layers stacked in the graphitic domains can be roughly estimated. The L_c and d_{002} values of the hard carbon were found to be 0.69 nm and 0.371 nm, respectively, indicating that the graphitic domain of the hard carbon is made up of 3–4 stacked graphene layers ($n = 0.690/0.371 + 1$). L_a value is 2.25nm.

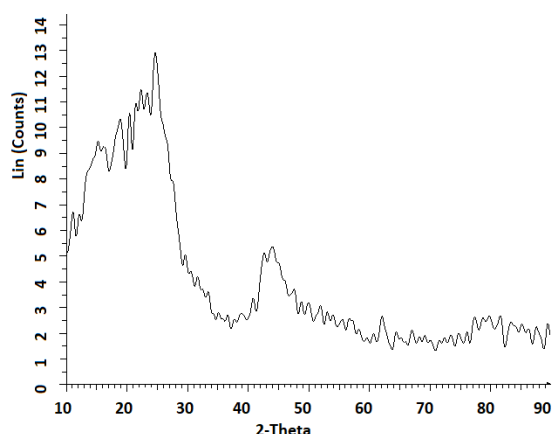


Fig.1. XRD pattern of the hard carbon carbonized at 1600°C

The Raman spectrum of the hard carbon is given in Fig.2. As shown in Fig.2, the spectrum shows two bands located at ~1340 and ~1584

cm⁻¹ corresponding to the defect induced D band representing the sp³ hybridized carbon atoms and the crystalline graphite G band representing sp² hybridized carbon atoms, respectively. The intensity ratio of the D band and G band (I_D/I_G) which is used to quantify the disorder degree of carbon materials was found to be 1.33. An I_D/I_G value greater than 1 implies the disordered nature of the carbon sheets and the associated unrepaired edge defects. The 2D peak at 2657.77 cm⁻¹ may also be used as a measure of disorder [19,20].

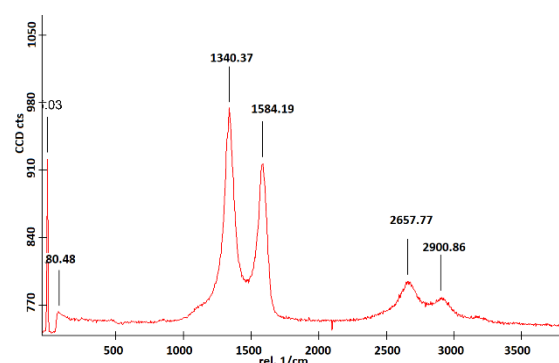


Fig.2. Raman spectrum of the hard carbon

A scanning electron microscope (SEM) image of the hard carbon is given Fig.3. As shown in the SEM image, the hard carbon consists of bulk particles and exhibits porous surface.

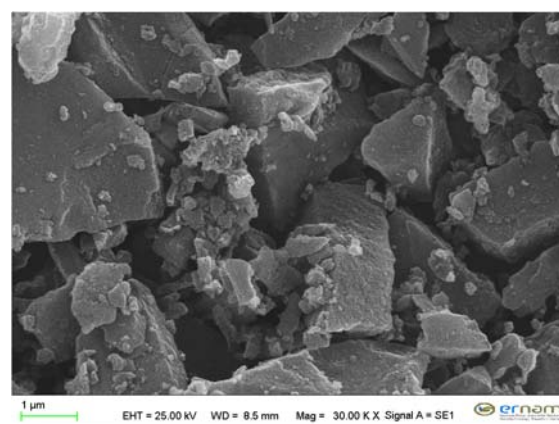


Fig.3. SEM micrograph of the hard carbon

Nitrogen adsorption–desorption isotherm for the hard carbon is given in Fig.4. As shown in Fig.4, the hard carbon demonstrates a typical type IV behavior, and the initial steep region indicates a certain amount of micropores [11] existing in the hard carbon with a Brunauer–Emmett–Teller (BET) surface area of 102 m² g⁻¹. The inset shows the pore size distribution calculated from the N₂ adsorption–

desorption isotherm using the Barrett–Joyner–Halenda (BJH) method. These distributions indicate the presence of both micropores and mesopores [13].

All the characterization results confirm that the nongraphitizable hard carbon pyrolyzed from the wood was obtained, which have micropores structure to facilitate the electrolyte penetration and provide sites for Na⁺ ion storage.

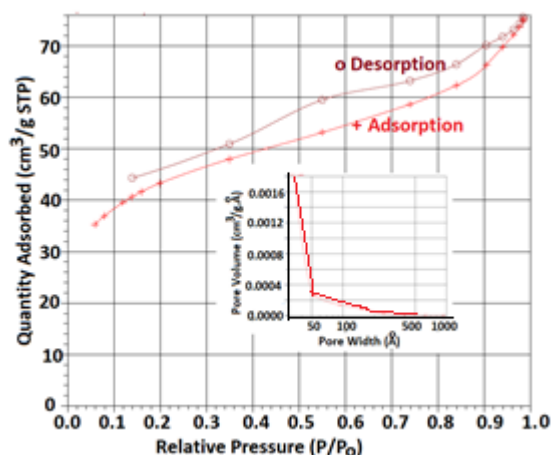


Fig.4. Nitrogen adsorption/desorption isotherm of the hard carbon

Galvanostatic charge/ discharge potential profiles of the hard carbon at different current rates are given in Fig.5. As reported before for hard carbon anodes in sodium ion batteries, the potential profile can be divided into two regions with a slope from 2.0 to ~0.15 V and a plateau close to 0 V. The sloping region corresponds to the insertion of Na⁺ ions intercalation into graphitic nanodomains along with the SEI formation, whereas the plateau region corresponds to the adsorption of Na ions into the hard carbon's nanovoids [23].

The first and second sodiation capacities are 320 and 235 mAh/g, respectively, yielding a high reversible capacity of 74%. This is one of the highest first-cycle reversible capacity value reported for hard carbon anodes in sodium ion batteries (see Table 1). The irreversible capacity loss in the first cycle is mainly due to the decomposition of the electrolyte that leads to the formation of a passivating solid electrolyte interphase (SEI) on the surface of the hard carbon.

The cycling performance of the hard carbon at different current rates is given in Fig.6. As seen from Fig.6, the decreases in specific capacity are observed at higher currents due to

the kinetic limitation of the hard carbon. After 134 cycles at 300 mA g⁻¹, 96.2% of the capacity for the second cycle at 0.1C remained.

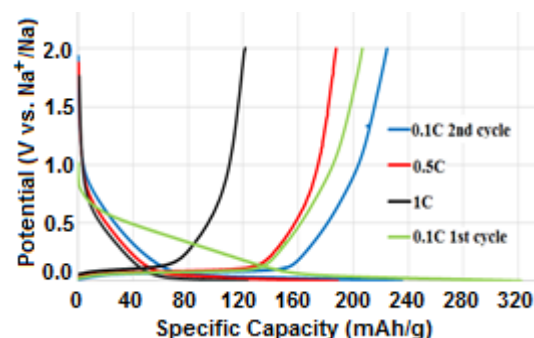


Fig.5. Galvanostatic charge/discharge curves of the hard carbon at 0.1C, 0.5C and 1.0C current densities (1.0C=300 mAh/g)

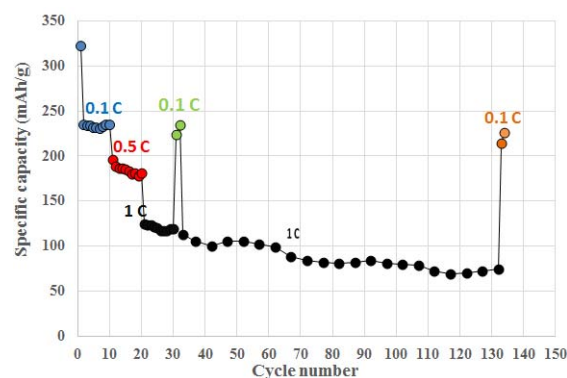


Fig.6. Cycling performance of the hard carbon at different current rates

Table 1. Electrochemical performances of reported carbon anode materials for SIBs.

Materials	nanoporous hard carbon	wood fibre derived carbon	commercially available hard carbon
Initial C.E.	77%	72%	78%
Cyclability (mAh/g)	289 at 0.02 A g ⁻¹ after 100 cycles	196 at 0.1A g ⁻¹ after 200 cycles	225 at 0.025 A g ⁻¹ after 100 cycles
Rate capability (mAh/g)	95 at 0.5 A g ⁻¹		
Reference	[24] 104	[25] 83	[26]

CONCLUSIONS

Hard carbon anode material has been successfully synthesized from pine wood via a simple, one-step pyrolysis process at 1600°C with the yield of 21%. The hard carbon demonstrates low initial irreversible capacity loss of 26%, the high reversible capacity of

~235 mA h g⁻¹ at a current density of 30 mA g⁻¹, and the capacity retention of ~96.2% after 134 cycles. This good performance highlights the potential of the pine wood pyrolyzed hard carbon for practical applications.

ACKNOWLEDGEMENTS

This work has been supported financially by Scientific Research Projects Unit of Erciyes University (with the Project Number FYL-2017-7621 and FBA-12-4031), which is gratefully acknowledged by the authors

REFERENCES

- [1] Yunming Li, Yaxiang Lu, Chenglong Zhao, Yong-Sheng Hu, Maria-Magdalena Titirici, Hong Li, Xuejie Huang, Liquan Chen. Recent advances of electrode materials for low-cost sodium-ion batteries towards practical application for grid energy storage. *Energy Storage Materials*, **7** 130–151 (2017).
- [2] M. Dahbi, N. Yabuuchi, K. Kubota, K. Tokiwa, S. Komaba. Negative electrodes for Na-ion batteries. *Phys. Chem. Chem. Phys.* **16**, 15007–15028 (2014).
- [3] C. Bommier, X.L. Ji. Recent Development on Anodes for Na-Ion Batteries. *Isr. J. Chem.* **55**, 486–507 (2015).
- [4] Hongshuai Hou, Xiaoqing Qiu, Weifeng Wei, Yun Zhang, Xiaobo Ji. Carbon Anode Materials for Advanced Sodium-Ion Batteries. *Adv. Energy Mater.*, 1602898 (2017).
- [5] Clement Bommier, Wei Luo, Wen-Yang Gao, Alex Greaney, Shengqian Ma, Xiulei Ji. Predicting capacity of hard carbon anodes in sodium-ion batteries using porosity measurements. *Carbon* **76**, 165-174 (2014).
- [6] F. Shen, H. Zhu, W. Luo, J. Wan, L. Zhou, J. Dai, B. Zhao, X. Han, K. Fu, L. Hu. Chemically Crushed Wood Cellulose Fiber towards High Performance Sodium-Ion Batteries. *ACS Appl. Mater. Interfaces* **7**, 23291–23296 (2015).
- [7] S. Komaba, W. Murata, T. Ishikawa, N. Yabuuchi, T. Ozeki, T. Nakayama, A. Ogata, K. Gotoh, K. Fujiwara. Electrochemical Na Insertion and Solid Electrolyte Interphase for Hard-Carbon Electrodes and Application to Na-Ion Batteries. *Adv. Funct. Mater.* **21**, 3859–3867 (2011).
- [8] Kun Wang, Yu Jin, Shixiong Sun, Yangyang Huang, Jian Peng, Jiahuan Luo, Qin Zhang, Yuegang Qiu, Chun Fang, Jiantao Han. Low-Cost and High-Performance Hard Carbon Anode Materials for Sodium-Ion Batteries. *ACS Omega* **2**, 1687–1695 (2017).
- [9] Fei Shen, Wei Luo, Jiaqi Dai, Yonggang Yao, Mingwei Zhu, Emily Hitz, Yuefeng Tang, Yanfeng Chen, Vincent L. Sprenkle, Xiaolin Li, Liangbing Hu. Ultra-Thick, Low-Tortuosity, and Mesoporous Wood Carbon Anode for High-Performance Sodium-Ion Batteries. *Adv. Energy Mater.*, **6**, 1600377 (2016).
- [10] Hongli Zhu, Fei Shen, Wei Luo, Shuze Zhu, Minhua Zhao, Bharath Natarajan, Jiaqi Dai, Lihui Zhou, Xiulei Ji, Reza S. Yassar, Teng Li, Liangbing Hu. Low temperature carbonization of cellulose nanocrystals for high performance carbon anode of sodium-ion batteries. *Nano Energy* **33**, 37–44 (2017).
- [11] F. Shen, H. Zhu, W. Luo, J. Wan, L. Zhou, J. Dai, B. Zhao, X. Han, K. Fu, L. Hu. Chemically Crushed Wood Cellulose Fiber towards High Performance Sodium-Ion Batteries. *ACS Appl. Mater. Interfaces* **7**, 23291–23296 (2015).
- [12] Kun Wang, Yu Jin, Shixiong Sun, Yangyang Huang, Jian Peng, Jiahuan Luo, Qin Zhang, Yuegang Qiu, Chun Fang, Jiantao Han. Low-Cost and High-Performance Hard Carbon Anode Materials for Sodium-Ion Batteries. *ACS Omega* **2**, 1687–1695 (2017).
- [13] Rohit Ranganathan Gaddam, Edward Jiang, Nasim Amiralian, Pratheep K. Annamalai, Darren J. Martin, Nanjundan Ashok Kumar X. S. Zhao. Spinifex nanocellulose derived hard carbon anodes for high-performance sodium-ion batteries. *Sustainable Energy Fuels* **1**, 1090–1097 (2017).
- [14] Li, Y. M.; Xu, S. Y.; Wu, X. Y.; Yu, J. Z.; Wang, Y. S.; Hu, Y. S.; Li, H.; Chen, L. Q.; Huang, X. J. Amorphous Monodispersed Hard Carbon Micro-Spherules Derived From Biomass as a High Performance Negative Electrode Material for Sodium-Ion Batteries. *J. Mater. Chem. A* **3**, 71–77 (2015).
- [15] Clement Bommier, Wei Luo, Wen-Yang Gao, Alex Greaney, Shengqian Ma, Xiulei Ji. Predicting capacity of hard carbon anodes in sodium-ion batteries using porosity measurements. *Carbon* **76**, 165-174 (2014).
- [16] Luo, W.; Bommier, C.; Jian, Z.; Li, X.; Carter, R.; Vail, S.; Lu, Y.; Lee, J.-J.; Ji, X. Low-Surface-Area Hard Carbon Anode for Na-Ion Batteries via Graphene Oxide as a Dehydration Agent. *ACS Appl. Mater. Interfaces* **7**, 2626–2631 (2015).
- [17] H. Wang, Z. Li, J.K. Tak, C.M.B. Holt, X. Tan, Z. Xu, B.S. Amirkhiz, D. Harfield, A. Anyia, T. Stephenson, D. Mitlin. Supercapacitors based on carbons with tuned porosity derived from paper pulp mill sludge biowaste. *Carbon* **57**, 317–328 (2013).
- [18] E.M. Lotfabad, J. Ding, K. Cui, A. Kohandehghan, W.P. Kalisvaart, M.

- Hazelton, D. Mitlin. High-Density Sodium and Lithium Ion Battery Anodes from Banana Peels. *ACS Nano* **8**, 7115–7129 (2014).
- [19] Jianyong Xiang, Weiming L, Congpu Mu, Jing Zhao, Bochong Wang. Activated hard carbon from orange peel for lithium/sodium ion battery anode with long cycle life. *Journal of Alloys and Compounds* **701**, 870-874 (2017).
- [20] Jia Ding, Huanlei Wang, Zhi Li, Alireza Kohandehghan, Kai Cui, Zhanwei Xu, Benjamin Zahiri, Xuehai Tan, Elmira Memarzadeh Lotfabad, Brian C. Olsen, David Mitlin. Carbon Nanosheet Frameworks Derived from Peat Moss as High Performance Sodium Ion Battery Anodes. *ACS Nano* **7**, 11004–11015, (2013).
- [21] Kun-lei Hong, Long Qie, Rui Zeng, Zi-qi Yi, Wei Zhang, Duo Wang, Wei Yin, Chao Wu, Qing-jie Fan, Wu-xing Zhang, Yun-hui Huang. Biomass derived hard carbon used as a high performance anode material for sodium ion batteries, *Mater. Chem. A* **2**, 12733-12738 (2014).
- [22] Weiming Lv, Fusheng Wen, Jianyong Xiang, Jing Zhao, Lei Li, Limin Wang, Zhongyuan Liu, Yongjun Tian. Peanut shell derived hard carbon as ultralong cycling anodes for lithium and sodium batteries. *Electrochimica Acta* **176**, 533–541 (2015).
- [23] Stevens, D. A.; Dahn, J. R. High Capacity Anode Materials for Rechargeable Sodium-Ion Batteries. *J. Electrochem. Soc.* **147**, 1271–1273 (2000).
- [24] S.R. Prabakar, J. Jeong, M. Pyo, Nanoporous hard carbon anodes for improved electrochemical performance in sodium ion batteries, *Electrochim. Acta* 2015, 161, 23.
- [25] F. Shen, H. Zhu, W. Luo, J. Wan, L. Zhou, J. Dai, B. Zhao, X. Han, K. Fu, L. Hu, Chemically Crushed Wood Cellulose Fiber towards High-Performance Sodium-Ion Batteries, *ACS Appl. Mater. Interfaces*, 2015, 7(41), 23291
- [26] S. Komaba, W. Murata, T. Ishikawa, N. Yabuuchi, T. Ozeki, T. Nakayama, A. Ogata, K. Gotoh, K. Fujiwara, Electrochemical Na Insertion and Solid Electrolyte Interphase for Hard-Carbon Electrodes and Application to Na-Ion Batteries, *Adv. Funct. Mater.* 2011, 21, 3859.